S©MR

СИБИРСКИЕ ЭЛЕКТРОННЫЕ
МАТЕМАТИЧЕСКИЕ ИЗВЕСТИЯ
Siberian Electronic Mathematical Reports
http://semr.math.nsc.ru
ISSN 1813-3304

Vol. 20, No. 2, pp. 144–145 (2025)
https://doi.org/10.33048/semi.2023.20.???

УДК 519.6
MSC 35Q92, 92D25

A FAMILY OF EQUILIBRIA AND LIMIT CYCLES IN A TRI-TROPHIC MODEL WITH TWO DELAYS

AHMAD ALMASRI AND **V.G. TSYBULIN**

Communicated by P.P. Petrov

Abstract: We investigate a delayed intraguild predation (IGP), or tri-trophic model that incorporates intraspecific competition and two distinct time delays, capturing gestation and handling effects. The system exhibits rich dynamics, including multistability and delay-induced oscillations. Using analytical techniques, we establish the existence of a continuous family of positive equilibria produced by cosymmetry. We investigate the stability of the equilibria from this family and define delays under which Poincaré–Andronov–Hopf bifurcations occur. The stability of the equilibria in the continuous family depends on the combination of time delays. Numerical simulations confirm the analytical predictions and illustrate how delays selectively destabilize parts of the equilibrium family. These findings highlight the complex interplay between time delays and multistability in shaping the dynamics of tri-trophic ecological systems.

Keywords: mathematical ecology, prey–predator–superpredator, differential equations, cosymmetry, multistability, delay.

Ahmad Almasri., V.G. Tsybulin., A family of equilibria and limit cycles in a tri-trophic model with two delays.

Received December, 23, 2025, Published December, 31, 2025.

1 Introduction

Intraguild predation (IGP) – a complex ecological interaction involving simultaneous competition and predation among species — plays a significant role in shaping community structure and biodiversity [1, 2]. Mathematical modeling of IGP systems has provided insights into the dynamic behaviors observed in natural ecosystems, including coexistence, extinction, and complex oscillatory patterns [3, 4, 5, 6]. Incorporating delays such as gestation periods, maturation times, and handling times into these models has enriched the understanding of the temporal dynamics and stability properties inherent to ecological interactions [7, 8].

The stability and asymptotic properties of solutions in biological systems with delay were analyzed using theory of functional differential equations [9, 10]. Specific applications to population dynamics, including predator-prey interactions and other living systems models, are investigated to establish conditions for local stability and characterize long-term behavior [11, 12, 13].

Time delays often induce complex phenomena such as stability switches, bifurcations, and chaos, which are critical for explaining irregular population fluctuations of the food chain models, for example IGP systems [14, 15, 16]. The interplay of delays and spatial effects can trigger intricate pattern formation and oscillatory behaviors [17, 18].

Vital problems require a study of the coexistence of species and the possibility of multiple scenarios for population system evolution. Research in physics and biology has yielded important results about multistability and its influence on dynamics and processes [19, 20, 21]. Multistability in predator-prey IGP systems was examined in [6, 22, 23] by using the cosymmetry theory [24]. While in [6] a family of equilibria was detected, an appearance of a family of oscillatory regimes was found in [23]. When the cosymmetry breaks, the destruction of a family of equilibria may be analyzed with the selective function approach [25].

However, the combined effect of multiple time delays on a system possessing a cosymmetry-induced family of equilibria remains largely unexplored. This work aims to bridge that gap by investigating how two distinct delays selectively influence the stability landscape of a tri-trophic IGP model with an inherent continuum of steady states.

We consider a delayed prey–predator–superpredator model that accounts for both intra- and interspecies interactions. The prey x grows logistically and is consumed by two predator populations y and z. The predator y hunts on x and is also consumed by the superpredator z. The system incorporates time delays τ_1 and τ_2 to describe gestation or handling times in predator

responses. The resulting system of delay differential equations is given by:

$$\begin{aligned}\frac{dx}{dt} &= x\big(1-x-y-z\big)\\ \frac{dy}{dt} &= -\mu_1 y+\eta_1\, x(t-\tau_1)\, y(t-\tau_1)-d_1 zy\\ \frac{dz}{dt} &= -\mu_2 z+\eta_2\, x(t-\tau_1)\, z(t-\tau_1)+d_2\, y(t-\tau_2)\, z(t-\tau_2).\end{aligned} \tag{1}$$

The first equation describes logistic growth of the prey population with limitations arising from both self-regulation and predation. The second and third equations model the delayed predator–prey interactions/ The reproduction of y depends on a time-lagged predation term $\eta_1\, x(t-\tau_1)\, y(t-\tau_1)$, while the dynamics of z involve two delayed interactions—one with the basal resource and another with the intermediate predator—via the terms $\eta_2\, x(t-\tau_1)\, z(t-\tau_1)$ and $d_2\, y(t-\tau_2)\, z(t-\tau_2)$, respectively. Parameters η_1, η_2 characterize the consumption of prey by predator and superpredator, d_1, d_2 define the consumption of a predator by the superpredator and μ_1, μ_2 are the natural mortalities for predator and superpredator.

This paper is organized as follows. We begin by identifying the equilibrium points of system (1) in Section 2. In Section 3, conditions for a nontrivial cosymmetry and parameters leading to the continuous family of equilibria are derived. The stability of these family members is also analyzed. Numerical simulations presented in Section 4 illustrate the dynamic behavior near the continuous family of equilibria. Different delay scenarios are listed, specifically the cases of a single non-zero delay ($\tau_1 = 0, \tau_2 \neq 0$ and $\tau_2 = 0, \tau_1 \neq 0$) and equal delays ($\tau_1 = \tau_2$). Finally, Section 5 provides a concluding discussion of the results.

2 Equilibrium points

System (1) has one trivial equilibrium $E_0 = (0, 0, 0)$, one axial equilibrium $E_1 = (1, 0, 0)$, irrespective of any parametric restriction, and some boundary equilibria.

The superpredator–absent equilibrium exists and is stable when $\eta_1 > \mu_1$

$$E_2 = \left(\frac{\mu_1}{\eta_1}, 1-\frac{\mu_1}{\eta_1}, 0\right).$$

Predator–absent equilibrium is stable when $\eta_2 > \mu_2$

$$E_3 = \left(\frac{\mu_2}{\eta_2}, 0, 1-\frac{\mu_2}{\eta_2}\right).$$

Under some conditions on parameters there exists the interior equilibrium $E_4 = (x_4, y_4, z_4)$. It corresponds to the scenario when all three interacting species will survive,

$$x_4 = \frac{1}{a}(-d_1 d_2 + d_1\mu_2 - d_2\mu_1), \quad a = -d_1 d_2 + d_1\eta_2 - d_2\eta_1,$$

$$y_4 = \frac{1}{a}(-d_1\mu_2 + d_1\eta_2 + \mu_1\eta_2 - \mu_2\eta_1),$$
$$z_4 = \frac{-1}{a}(-d_2\mu_1 + d_2\eta_1 + \mu_1\eta_2 - \mu_2\eta_1).$$

To analyze the local stability of the equilibria of the delay system, we provide linearization of the system on the steady state (x_4, y_4, z_4). Setting the perturbations as $u = (u_1, u_2, u_3)$, $x(t) = x_4 + u_1(t)$, $y(t) = y_4 + u_2(t)$, $z(t) = z_4 + u_3(t)$, the linearized system has the form

$$\frac{d\mathbf{u}}{dt} = J_0\,\mathbf{u}(t) + J_{\tau_1}\,\mathbf{u}(t-\tau_1) + J_{\tau_2}\,\mathbf{u}(t-\tau_2) \tag{2}$$

where the instantaneous Jacobian matrix J_0 is

$$J_0 = \begin{pmatrix} 1 - 2x_4 - y_4 - z_4 & -x_4 & -x_4 \\ 0 & -\mu_1 - d_1 z_4 & -d_1 y_4 \\ 0 & 0 & -\mu_2 \end{pmatrix} \tag{3}$$

and the delay matrices J_{τ_1} and J_{τ_2} correspond to terms involving delayed variables:

$$J_{\tau_1} = \begin{pmatrix} 0 & 0 & 0 \\ \eta_1 y_4 & \eta_1 x_4 & 0 \\ \eta_2 z_4 & 0 & \eta_2 x_4 \end{pmatrix}, \quad J_{\tau_2} = \begin{pmatrix} 0 & 0 & 0 \\ 0 & 0 & 0 \\ 0 & d_2 z_4 & d_2 y_4 \end{pmatrix}. \tag{4}$$

The characteristic equation determining stability is given by

$$\det\left(\sigma I - J_0 - e^{-\sigma\tau_1} J_{\tau_1} - e^{-\sigma\tau_2} J_{\tau_2}\right) = 0, \tag{5}$$

Here, I denotes the 3×3 identity matrix, and σ is the spectral parameter. The exponential terms $e^{-\sigma\tau_1}$ and $e^{-\sigma\tau_2}$ incorporate the effects of time delays in the feedback loops.

At the extinction equilibrium E_0, the delay-dependent Jacobian matrices J_{τ_1} and J_{τ_2} are null. The characteristic equation (5) reduces to $\det(\sigma I - J_0) = 0$, yielding the eigenvalues directly:

$$\sigma_1 = 1, \quad \sigma_2 = -\mu_1, \quad \sigma_3 = -\mu_2.$$

Since $\sigma_1 = 1 > 0$, the equilibrium E_0 is unstable for all parameter values and delays $\tau_1, \tau_2 \geq 0$.

Lemma 1. *The equilibrium E_1 is locally asymptotically stable for all delays $\tau_1, \tau_2 > 0$ when $\mu_1 > \eta_1$, $\mu_2 > \eta_2$.*

Proof. At the predator-free equilibrium E_1, the Jacobian matrix J_{τ_2} is zero. The characteristic equation (5) takes the form:

$$(\sigma + 1)g(\sigma) = 0, \qquad g(\sigma) = \left(\sigma + \mu_1 - \eta_1 e^{-\sigma\tau_1}\right)\left(\sigma + \mu_2 - \eta_2 e^{-\sigma\tau_1}\right)$$

The first factor gives $\sigma = -1$. The stability of E_1 is thus governed by the two transcendental equations associated with the predator (y) and superpredator (z) populations. Here, $\mu_1, \mu_2, \eta_1, \eta_2 > 0$ and $\tau_1 > 0$. We now analyze the distribution of zeros of $g(\sigma)$. When $\mu_1 > \eta_1$, $\mu_2 > \eta_2$. All roots of $g(\sigma)$ have negative real parts. Specifically, there exists a unique negative real root, and

all complex roots satisfy $\Re(\sigma) < 0$. Therefore, the equilibrium E_1 is locally asymptotically stable for all delays $\tau_1, \tau_2 \geq 0$. Conversely, if $\mu_1 < \eta_1$ or $\mu_2 < \eta_2$. The function $g(\sigma)$ possesses a positive real root. Consequently, E_1 is unstable. □

Remark 1. *when $\mu_1 = \eta_1$ ($\mu_2 = \eta_2$), the equilibrium E_2 (E_3) branches off from E_1 in a transcritical bifurcation.*

The stability analysis for other equilibria may be done only for specific values of parameters. For example, the case $\tau_1 = \tau_2$ was considered for the Bazykin model in [26], where no continuous family of equilibria was found. Furthermore, the study in [6], the study with $\tau_i = 0$ $(i = 1, 2)$ revealed multistability, demonstrating that multiple stable states can exist under additional parameter conditions.

3 Cosymmetry

Cosymmetry [24] means the appearance of a family of steady states (extreme multistability) in the system of autonomous first-order differential equations. Cosymmetry is also a non-trivial vector field orthogonal to the right-hand side of the system (1). The nontrivial cosymmetry of the system produces a continuous family of equilibria with a stability spectrum that varies along the family.

Proposition 1. *Under the parameter conditions:*

$$\mu_2 = d_2\left(1 + \frac{\mu_1}{d_1}\right), \quad \eta_2 = d_2\left(1 + \frac{\eta_1}{d_1}\right). \tag{6}$$

the system (1) has a cosymmetry

$$L = \left[yz, -\frac{1}{d_1}xz, \frac{1}{d_2}xy\right]^T \tag{7}$$

and possesses a continuous family of equilibria given by

$$Q = \left\{x \in \left[\frac{\mu_1}{\eta_1}, \frac{d_1 + \mu_1}{d_1 + \eta_1}\right], \quad y = 1 + \frac{\mu_1}{d_1} - (1 + \frac{\eta_1}{d_1})x, \quad z = \frac{\eta_1 x - \mu_1}{d_1}\right\} \tag{8}$$

Proof. For $\tau_i = 0$, multiplying the right side of system (1) on cosymmetry (7), we get:

$$\begin{aligned} < F, L >= xyz\Big[1 - x - y - z + c_1(-\mu_1 + \eta_1 x - d_1 z) \\ + c_2(-\mu_2 + \eta_2 x + d_2 y)\Big] \end{aligned} \tag{9}$$

After substitution (7) to (9) and simplification, we obtain $< F, L >= 0$. This means that the vector function L is orthogonal to the right-hand side of the system (1), i.e., L is a cosymmetry of the system. □

It should be noted that the family of equilibria includes the boundary equilibrium E_2 ($x = \frac{\mu_1}{\eta_1}$) and the equilibrium E_3 ($x = \frac{d_1+\mu_1}{d_1+\eta_1}$).

Proposition 2. *System (1) under conditions (6) and $\tau_1 = \tau_2 = 0$ has a continuous family of stable equilibria (8).*

Proof. In the absence of delays ($\tau_1 = \tau_2 = 0$) and under conditions (6), the characteristic equation (5) reduces to

$$\det\left(\sigma I - J_0 - J_{\tau_1} - J_{\tau_2}\right) = 0, \tag{10}$$

and the stability of the family of equilibria is determined by the eigenvalues of the matrix $J = J_0 + J_{\tau_1} + J_{\tau_2}$. The Jacobian matrix at the family of equilibria (8) is given by:

$$J = \begin{bmatrix} -x & x & -x \\ y\eta_1 & 0 & -yd_1 \\ z\eta_2 & zd_2 & 0 \end{bmatrix} \tag{11}$$

The characteristic equation for J_Q is written as:

$$\sigma^3 + A_2\sigma^2 + A_1\sigma = 0$$

where

$$\begin{aligned} A_2 &= x \\ A_1 &= \eta_1 xy + \eta_2 xz + d_1 d_2 yz \end{aligned} \tag{12}$$

The zero root $\sigma_1 = 0$ corresponds to neutral stability along the family Q. Since $A_1, A_2 > 0$, the equilibria of the family Q are stable. □

The family of equilibria (8) exists for any values of τ_1 and τ_2. Notably, any point $x \in \left[\frac{\mu_1}{\eta_1}, \frac{d_1+\mu_1}{d_1+\eta_1}\right]$ constitutes an equilibrium, and it can be realized through the appropriate choice of initial history functions on $t \in [-\tau_{\max}, 0]$, where $\tau_{\max} = \max(\tau_1, \tau_2)$. For nonzero delays τ_i ($i = 1, 2$), the stability analysis of equilibria belonging to the family requires numerical computations. Only a few special cases can be treated analytically.

Lemma 2. *For the case $\tau_1 = 0$, the boundary equilibria E_2 and E_3 are locally asymptotically stable for any $\tau_2 > 0$.*

Proof. Under the cosymmetry conditions in (6), the characteristic equation at the boundary equilibrium E_2 (where the superpredator is absent, $z = 0$) is:

$$\sigma + d_2 y(1 - e^{-\sigma\tau_2}) = 0. \tag{13}$$

We first observe that this equation admits no real roots $\sigma > 0$ or $\sigma < 0$. Assume $\sigma = iw$ with $\omega > 0$. Separating real and imaginary parts leads to

$$d_2 y(1 - \cos(w\tau_2)) = 0, \qquad w + d_2 y \sin(w\tau_2) = 0. \tag{14}$$

Since $d_2 y > 0$, the first equality implies $\cos(w\tau_2) = 1$, hence $w\tau_2 = 2\pi k$, $k \in \mathbb{Z}$. Substituting into the second equation (14) yields $\omega = 0$, contradicting

$w > 0$. Therefore, there exist no nonzero purely imaginary roots $\sigma = i\omega$ of (13). The only root on the imaginary axis is $\sigma = 0$.

At the boundary E_3 (where the predator is absent, $y = 0$), the characteristic equation $\sigma(\sigma^2 + x\sigma + \eta_2 xz) = 0$, which is independent of τ_2. Consequently, the stability of this boundary equilibrium is unaffected by the delay τ_2. □

Furthermore, we present numerical results for specific parameter values that demonstrate a scenario of partial instability within the family of equilibria.

4 Numerical analysis

To investigate the system's dynamics, we use MATLAB with the DDE-BIFTOOL package [27] for numerical continuation and bifurcation analysis. This approach enables a detailed exploration of its response to variations in the delay parameters. The values of the parameters are taken as: $\mu_1 = 1$, $\eta_1 = 10$, $d_1 = 1$, $d_2 = 1$, and μ_2, η_2 satisfying (6).

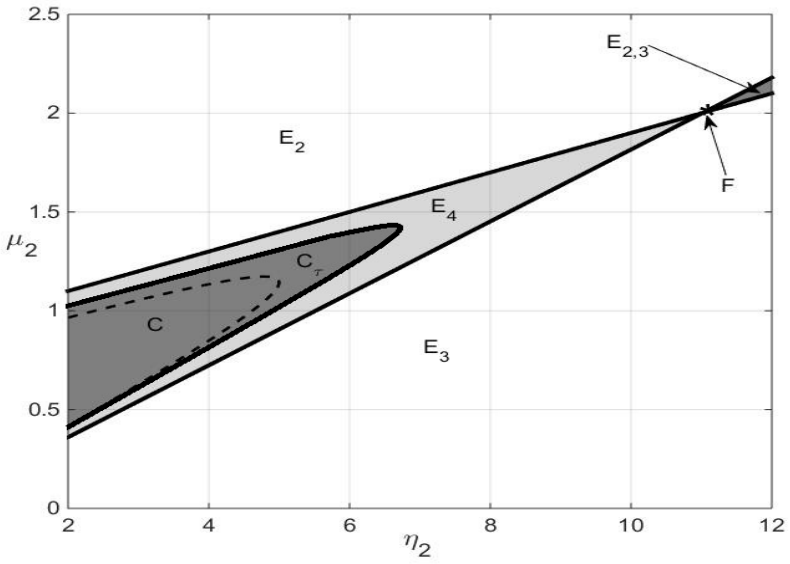

FIG. 1. Two-parameter bifurcation diagram with respect to η_2 and μ_2, E_j $(j = 2, 3, 4)$ – regions of monostability, $E_{2,3}$ – the region of bistability, C – the region of limit cycles without delay, C_τ – the region of limit cycles with delay $\tau_1 = \tau_2 = 0.05$, point F corresponds to the family of equilibria; $\mu_1 = 1$, $\eta_1 = 10$, $d_1 = 1$, $d_2 = 1$.

The regime map on the parameter plane η_2 and μ_2 is displayed in Fig. 1. Symbol E_j marks the stability domain for the equilibrium E_j, $j = 2, 3, 4$. Stable equilibria E_2 and E_3 coexist for the parameter values within the bistability region $E_{2,3}$. The domains E_2, E_3, E_4, and E_{23} share a point

F, which corresponds to the family of equilibria. The symbol C denotes the region of values for which limit cycles exist for $\tau_1 = \tau_2 = 0$. Fig. 1 also shows the region C_τ obtained through a computational experiment for $\tau_1 = \tau_2 = 0.05$. This region C_τ represents the parameters (η_2, μ_2) for which the equilibrium E_4 is unstable and stable limit cycles exist. When the delay increases, the size of region C_τ becomes larger. Furthermore, each point within C_τ corresponds to a unique limit cycle.

For the non-delayed case $\tau_1 = \tau_2 = 0$, the family Q (8) (point F in Fig. 1) contains only stable equilibria, see Propositions 1 and 2. Furthermore, we will demonstrate that, under the influence of delay, some parts of the family become unstable, and the entire family may contain unstable equilibria.

i	$Q_i(x_i, y_i, z_i)$	$\tau_2 = 0$	$\tau_2 = 0.1$	$\tau_2 = 0.3$
1	$Q_1(0.11, 0.77, 0.12)$	0.140	0.134	0.130
2	$Q_2(0.12, 0.64, 0.23)$	0.146	0.137	0.133
3	$Q_3(0.14, 0.51, 0.35)$	0.151	0.142	0.140
4	$Q_4(0.15, 0.38, 0.47)$	0.157	0.149	0.149
5	$Q_5(0.16, 0.25, 0.58)$	0.163	0.157	0.159
6	$Q_6(0.17, 0.12, 0.7)$	0.168	0.164	0.167

ТАБЛИЦА 1. Critical values τ_1^{crit} for several equilibria from the family Q under different delay τ_2; $\mu_1 = 1$, $\eta_1 = 10$, $d_1 = 1$, $d_2 = 1$.

Table 1 presents six points selected from the family of equilibria (8), where all three species coexist (prey–predator–superpredator). For these points, we compare the bifurcation threshold τ_1^{crit} across different delay scenarios: $\tau_2 = 0$, $\tau_2 = 0.1$ and $\tau_2 = 0.3$. The analysis shows that the parameter τ_1^{crit} increases monotonically with the index i (number of an equilibrium Q_i). Consequently, for lower values of i, where τ_1 remains below a critical threshold τ_1^{crit}, the entire family of equilibrium points is stable. However, stability across the family Q varies with τ_1^{crit}—while some parts remain stable, others undergo instability. These critical values determine exactly when oscillations appear in the system, illustrating how the delays τ_1 and τ_2 influence the onset of biological dynamics.

When $\tau_1 = 0$ and $\tau_2 \neq 0$, the family Q (8) contains only stable equilibria. Fig. 2a shows that the trajectories converge oscillatory toward the family of equilibria (black line E_2E_3) for different initial conditions when $\tau_1 = 0$, $\tau_2 = 1$. For $\tau_2 = 2$, the trajectories exhibit faster convergence to the equilibrium family compared to $\tau_2 = 1$ (see Fig. 2b).

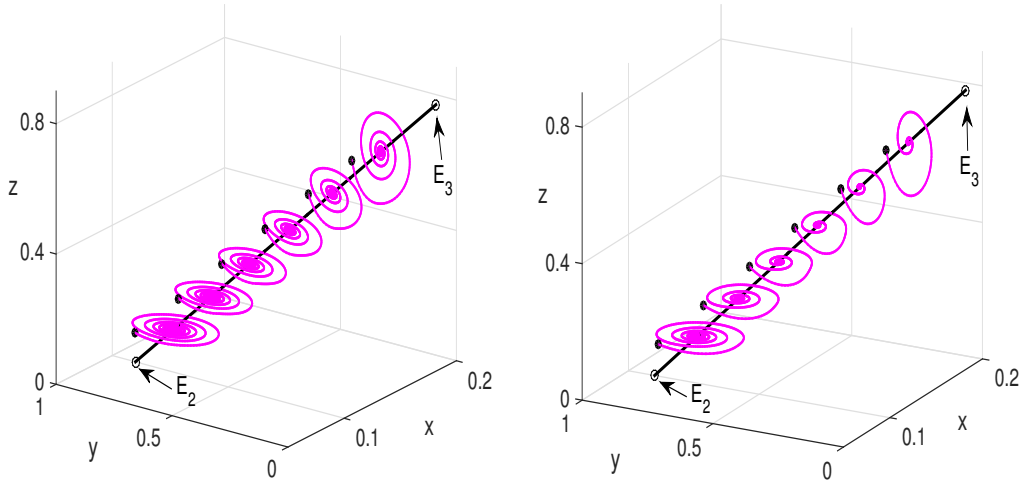

FIG. 2. Convergence to equilibria of the family Q (black line) from different initial points for $\tau_1 = 0$. *a*) $\tau_2 = 1$, *b*) $\tau_2 = 2$; $\mu_1 = 1$, $\eta_1 = 10$, $d_1 = 1$, $d_2 = 1$.

For system (1) with $\tau_2 = 0$, $\tau_1 \neq 0$ the stability of the equilibria Q_1 (curve 2) and Q_5 (curve 3) is analyzed using their eigenvalues (see Fig. 3). The critical bifurcation points τ_1^{crit} are marked in red. Both Q_1 (curve 2) and Q_5 (curve 3) are stable for delays $\tau_1 < \tau_1^{\text{crit}}$ and lose stability via a Poincaré–Andronov–Hopf bifurcation when τ_1 exceeds this critical value. For $\tau_1 = \tau_1^{\text{crit}}$, it gives a periodic solution.

For $\tau_2 = 0$, the Table 1 shows that the critical value τ_1^{crit} varies from 0.14 to 0.168. So, in the case of $\tau_1 = 0.151$, we obtain stable and unstable equilibria, as well as a periodic solution (see Fig. 4). Fig. 4a shows the time evolution of the superpredator population for initial points from vicinity of the family of equilibria Q. The results demonstrate three distinct behaviors: a stable equilibrium at $z = 0.7$ and 0.58, an unstable equilibrium at $z = 0.23$, and a periodic solution $z = 0.35$. Fig. 4b demonstrates that trajectories converge oscillatorily towards the family of equilibria (black line E_2E_3) when $z = 0.7$ and 0.58. A limit cycle is realized at $z = 0.35$, while growing oscillations at $z = 0.23$.

For the case $\tau_1 = \tau_2 = \tau$, we find that the bifurcations for the equilibria $(Q_i, i = 1, .., 6)$ occur at critical values $\tau^{\text{crit}} = 0.133, 0.135, 0.14, 0.147, 0.155, 0.163$, respectively. When $\tau_1 = \tau_2 = 0.1$, all equilibrium points Q_i are stable, see Fig. 5. The principal eigenvalues constituting the stability spectrum for these solutions Q_i have been computed and are tabulated on the right of Fig. 5.

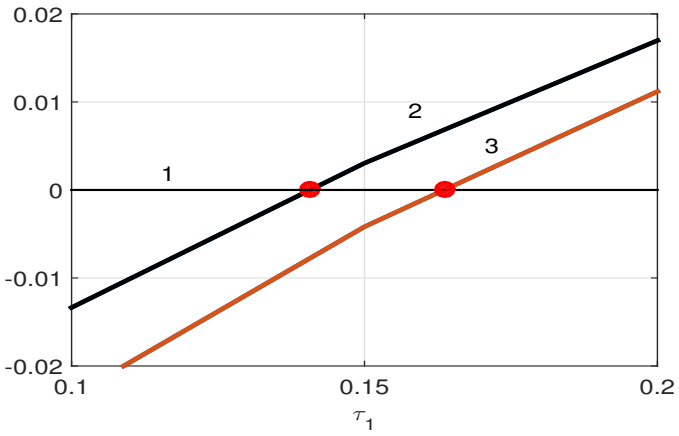

FIG. 3. Dependence upon τ_1 of real parts of the eigenvalues for Jacobian at equilibria Q_1 (curves 1, 2) and Q_5 (curves 1, 3), $\tau_2 = 0$; $\mu_1 = 1$, $\eta_1 = 10$, $d_1 = 1$, $d_2 = 1$.

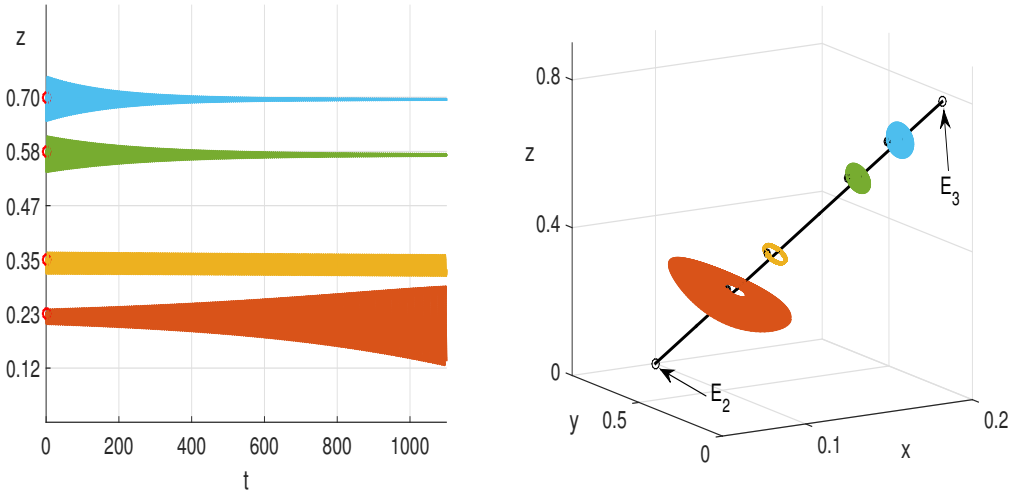

FIG. 4. Dynamics scenarios for System (1) with $\tau_1 = 0.151$, $\tau_2 = 0$, under cosymmetry conditions (6) from different initial points; $\mu_1 = 1$, $\eta_1 = 10$, $d_1 = 1$, $d_2 = 1$.

The destabilizing effect of the delay τ_1 on the stability of family is vividly demonstrated in Fig. 6. This figure captures the phenomenon of multistability – the coexistence of multiple attractors for a single set of parameters. It is a direct consequence of cosymmetry. We fix the delay $\tau_1 = \tau_2 = 0.14$ and select different points along the family of equilibria Q (see. Table 1). This

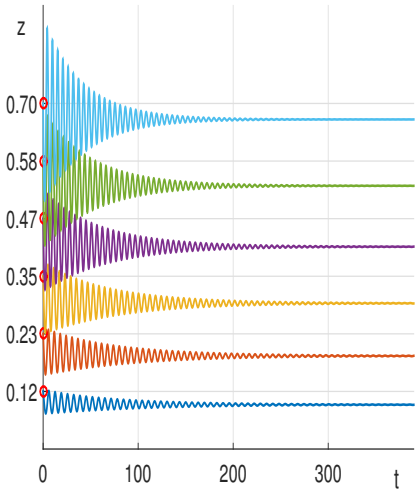

Q_i	σ_1	$\sigma_{2,3}$
Q_1	-7.870×10^{-8}	$-0.011 \pm 0.975i$
Q_2	-1.172×10^{-7}	$-0.012 \pm 1.031i$
Q_3	-1.294×10^{-7}	$-0.014 \pm 1.074i$
Q_4	-1.217×10^{-7}	$-0.017 \pm 1.108i$
Q_5	-9.694×10^{-8}	$-0.020 \pm 1.133i$
Q_6	-5.635×10^{-8}	$-0.024 \pm 1.151i$

FIG. 5. Convergence to equilibria of the family Q at $\tau_1 = \tau_2 = 0.1$ for different initial conditions (left). Main values of the stability spectrum for equilibria (right); $\mu_1 = 1$, $\eta_1 = 10$, $d_1 = 1$, $d_2 = 1$.

specific value τ is supercritical for some equilibria and subcritical for others, allowing us to observe multiple dynamical regimes simultaneously.

Fig. 6a shows the time series of the superpredator density (z). It reveals three distinct outcomes based solely on initial conditions. At high z, the trajectories starting near the family of Q (e.g., $z = 0.7$ or 0.58) converge with oscillations to stable equilibria. This indicates that for these population densities, the system is resilient and returns to steady coexistence. The trajectory starting near $z = 0.47$ evolves to a persistent, stable periodic oscillation. Here we see a Poincaré–Andronov–Hopf bifurcation, where a stable limit cycle occurs. A trajectory starting near a low-density superpredator equilibrium ($z = 0.23$) deviates away from it. This indicates that this specific equilibrium is unstable one, making coexistence at these population levels unsustainable for the given parameters.

The location of the various trajectories and objects is shown in Fig. 6b The continuous family of equilibria Q is represented by the solid black line connecting the boundary equilibria E_2 and E_3. The trajectories show how the dynamics are determined by its initial state. One can see convergence to stable equilibria on the family's line, while others are attracted to the isolated limit cycle or tend to the equilibrium E_2.

In summary, Fig. 6 provides a compelling visual representation of how the delay τ selectively destabilizes specific segments of the continuous family of equilibria, leading to a complex landscape where stable and unstable points as well as periodic solutions coexist. This underscores the critical importance

of the initial predator-superpredator proportion in the long-term scenario of delayed intraguild predation systems.

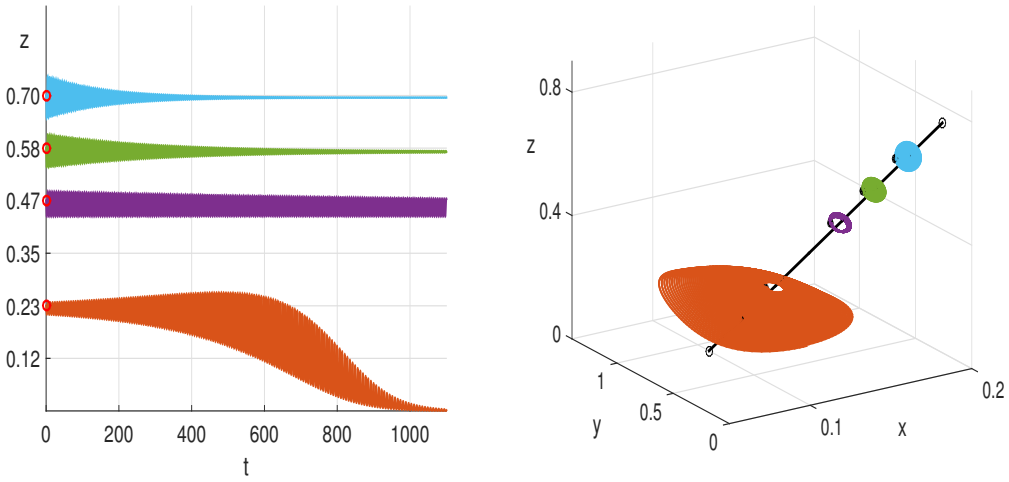

FIG. 6. Dynamics scenarios under cosymmetry conditions (6) and delay $\tau_1 = \tau_2 = 0.14$. Dependence of the superpredator population on time (a) and trajectories (b) originating from different initial conditions near the family of equilibria Q; $\mu_1 = 1$, $\eta_1 = 10$, $d_1 = 1$, $d_2 = 1$.

Figure 7 shows that a sufficiently large time delay can completely destabilize the entire continuous family of equilibria, leading to the emergence of persistent oscillatory dynamics. The figure 7a depicts a trajectory (shown in red), originating from an initial condition near equilibrium Q_6 of the family Q. However, unlike in scenarios with smaller delays, where trajectories converge to stable equilibria of the family, this trajectory evolves into a stable limit cycle without a superpredator. In addition to this cycle, there is also a prey–superpredator cycle (without predator), see both cycles in figure 7b.

This behavior occurs because the chosen delay $\tau = 0.2$ exceeds the critical bifurcation value τ^{crit} for all equilibria in the family Q. As detailed in Table. 1, the critical values for the family points Q_1 to Q_6 when $\tau_1 = \tau_2$ lie in the interval $[0.134, 0.164]$. Since $\tau = 0.2$ is greater than all these thresholds, every equilibrium point on the family Q has lost its stability via a Poincaré–Andronov–Hopf bifurcation. Thus, Figure 7 illustrates the powerful destabilizing role of time delays, showing that beyond a critical threshold, they can destroy the multistability in a cosymmetric system and produce oscillatory regimes in a lower-dimensional subspace.

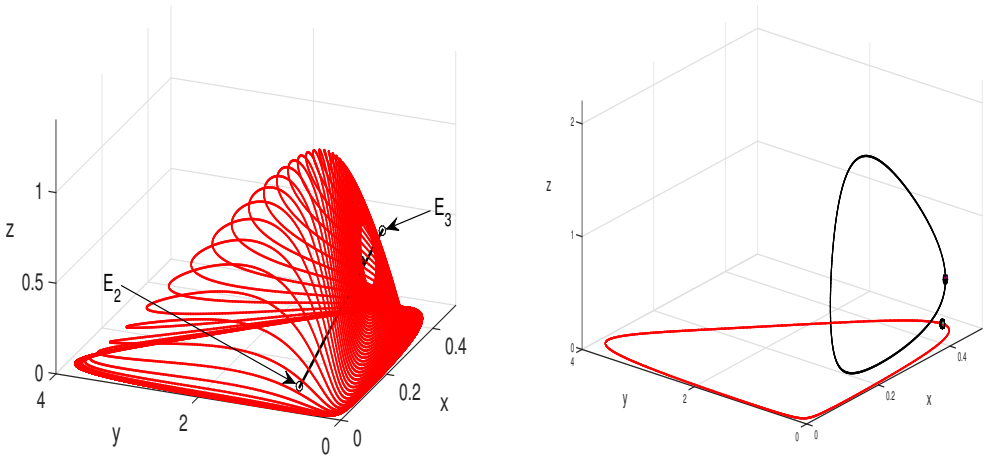

a b

FIG. 7. Phase portrait of the system (1) for $\tau_1 = \tau_2 = 0.2$. *a*) Convergence to the limit cycle in the absence of the superpredator, *b*) shows the superpredator-free limit cycle (red) and the predator-free limit cycle (black), the solid black line E_2E_3 represents the continuous family of equilibria Q; $\mu_1 = 1$, $\eta_1 = 10$, $d_1 = 1$, $d_2 = 1$.

5 Conclusions

This study presents an analytical and numerical investigation of the dynamics of a tri-trophic intraguild predation model with two distinct time delays. The main focus is on a family of equilibria that occurs in multi-species ecological models when certain additional conditions are met for parameters that characterize predator behavior. This results in a cosymmetrical continuous family of equilibrium points. Interaction between time delays and other parameters produces a wide range of dynamic behaviors, primarily including multistability and periodic oscillations induced by delays.

Our results concern the role of time delays in governing the stability of the family of equilibria:

- The delay τ_2 (associated with the superpredator's handling time) is non-destabilizing; the entire family of equilibria remains stable for any $\tau_2 > 0$ when $\tau_1 = 0$.
- In contrast, the delay τ_1 (associated with predator gestation) acts as a critical bifurcation parameter. The system undergoes a Poincaré–Andronov–Hopf bifurcation when τ_1 exceeds a threshold value τ_1^{crit}, moving from stable coexistence to persistent periodic oscillations. This shows how inherent biological lags can drive population cycles in complex food webs.

- The scenario of equal delays ($\tau_1 = \tau_2 > 0$) also yields a Poincaré–Andronov–Hopf bifurcation at a critical value, confirming that delays can synergistically destabilize the system.

Critical delay thresholds were calculated throughout the family of equilibria, revealing that stability does not degrade uniformly. As a result, stable and unstable equilibrium states coexist under identical parameter conditions, underscoring the system's multistable nature. Numerical simulations confirm this complex behavior, visually demonstrating trajectories that converge to stable points or form limit cycles.

Biologically, this reflects the ability of an ecological community to sustain multiple stable structures under the same set of environmental conditions. This phenomenon can be considered a manifestation of the ecological plasticity of the system, allowing it to adapt to environmental variations. These findings are consistent with the established ecological concept that the history of a community influences its state and dynamics following changes in external conditions.

References

[1] A.D. Bazykin, *Nonlinear Dynamics of Interacting Populations*, World Scientific, River Edge, 1998. MR1635219

[2] R. D. Holt, G. A. Polis, *A theoretical framework for intraguild predation*, Am. Naturalist, **149**:4 (1997), 745–764.

[3] D. Sen, S. Ghorai, M. Banerjee, *Complex dynamics of a three species prey-predator model with intraguild predation*, Ecol. Complex, **34** (2018), 9–22.

[4] H. Wei, *A mathematical model of intraguild predation with prey switching*, Math. Comput. Simul., **165** (2019), 107–118. Zbl 7316739

[5] G. Ble, V. Castellanos, I.L.Hernandez, *Stable limit cycles in an intraguild predation model with general functional responses*, Math. Methods Appl. Sci., **45**:4 (2022), 2219–2233. Zbl 1533.37170

[6] A. Almasri, V.G. Tsybulin, *A dynamic analysis of a prey-predator-superpredator system: a family of equilibria and its destruction*, Computer Research and Modeling, **15**:6 (2023), 1603–1617.

[7] G. Fan, G.S.K. Wolkowicz, *Chaotic dynamics in a simple predator–prey model with discrete delay*, arXiv preprint, (2020), arXiv:2007.16140.

[8] A. Frank, S. Subbey, M. Kobras, H. Gjøsæter, *Population dynamic regulators in an empirical predator-prey system*, Journal of Theoretical Biology, **527** (2021), Article ID 110814

[9] V.B. Kolmanovskii, A.D. Myshkis, *Introduction to the Theory and Applications of Functional Differential Equations*, Kluwer Academic Publishers, Dordrecht, 1999.

[10] R.P. Agarwal, L. Berezansky, E. Braverman, A. Domoshnitsky, *Nonoscillation Theory of Functional Differential Equations with Applications*, Springer, New York, 2012.

[11] V.V. Malygina, M.V. Mulyukov, N.V. Pertsev, *On the local stability of a population dynamics model with delay*, Siberian Electronic Mathematical Reports, **11** (2014), 951–957.

[12] K.K. Loginov, N.V. Pertsev, *Asymptotic Behavior of Solutions to a Delay Integro-Differential Equation Arising in Models of Living Systems*, Siberian Advances in Mathematics, **31**:2 (2021), 131–146.

[13] M. A. Skvortsova, T. Yskak, *Asymptotic behavior of solutions in one predator–prey model with delay*, Siberian Math. J., **62**:2 (2021), 324–336.
[14] F.A. Rihan, H. J. Alsakaji, C. Rajivganthi, *Stability and Hopf Bifurcation of Three–Species Prey–Predator System with Time Delays and Allee Effect*, Complexity, **2020**:1 (2020), Article ID 7306412
[15] F.A. Rihan, H. J. Alsakaji, *Stochastic delay differential equations of three-species prey-predator system with cooperation among prey species*, Discrete and Continuous Dynamical Systems-S, **15**:2 (2022), 245–263.
[16] R. Shi, Z. Hu, *Dynamics of three-species food chain model with two delays of fear*, Chinese Journal of Physics., **77** (2022), 678–698.
[17] R. Han, B. Dai, *Spatiotemporal dynamics and spatial pattern in a diffusive intraguild predation model with delay effect*, J. Appl. Math. Comput, **312** (2017), 177–201.
[18] D. Zhang, B. Dai, *A free boundary problem for the diffusive intraguild predation model with intraspecific competition*, Journal of Mathematical Analysis and Applications., **474**:1 (2019), 381–412.
[19] AN. Pisarchik, U. Feudel, *Control of multistability*, Phys Rep, **540**:4 (2014), 167–218. Zbl 1357.34105
[20] I. Bashkirtseva, AN. Pisarchik, L. Ryashko, *Multistability and stochastic dynamics of Rulkov neurons coupled via a chemical synapse*, Communications in Nonlinear Science and Numerical Simulation, **125** (2023), Article ID 107383. Zbl 1527.92014
[21] V.N. Govorukhin, V.G. Tsybulin, *Dynamics of mechanical system with curve of equilibria: cosymmetry and multistability*, Int. J. Bifurcation and Chaos, **32**:16 (2022), Article ID 2230037.
[22] A. Almasri, V.G. Tsybulin, *Multistability and dynamic scenarios in the prey–predator–superpredator model*, Siberian Electronic Mathematical Reports, **21**:2 (2024), 771–788.
[23] A. Almasri, B. H. Nguyen, V.G. Tsybulin, *Continuous families of equilibria and periodic regimes in the prey–predator–superpredator system*, Vestnik Udmurtskogo Universiteta. Matematika. Mekhanika. Komp'yuternye Nauki, **35**:3 (2025), 337–355.
[24] V.I. Yudovich, *Cosymmetry, degeneration of solutions of operator equations, and onset of a filtration convection*, Math. Notes, **49**:5 (1991), 540–545. Zbl 0747.47010
[25] V.I. Yudovich, *Bifurcations under perturbations violating cosymmetry*, Dokl. Phys., **49** (2004), 522—526.
[26] Z. Li, B. Dai, *Global dynamics of delayed intraguild predation model with intraspecific competition*, International Journal of Biomathematics, **11**:8 (2018), 1850116.
[27] K. Engelborghs, T. Luzyanina, D. Roose, *Numerical bifurcation analysis of delay differential equations using DDE-BIFTOOL*, ACM Transactions on Mathematical Software (TOMS), **28** (2002), 1–21.

Ahmad Almasri
Southern Federal University,
Milchakova St., 8-A,
344006, Rostov on Don, Russia
Email address: ahmal6398@gmail.com

V.G. Tsybulin
Southern Federal University,
Milchakova St., 8-A,
344006, Rostov on Don, Russia
Email address: vgcibulin@sfedu.ru